

RESEARCH ARTICLE

Differential regulation of innate immune cytokine production through pharmacological activation of Nuclear Factor-Erythroid-2-Related Factor 2 (NRF2) in burn patient immune cells and monocytes

Timothy K. Eitas¹, Wesley Stepp², Lucas Sjeklocha², Clayton Long², Caitlin Riley², James Callahan³, Yolanda Sanchez³, Peter Gough¹, Laquanda Knowlin², David van Duin⁴, Shiara Ortiz-Pujols², Samuel Jones², Robert Maile², Zhi Hong⁵, Scott Berger^{1*}, Bruce Cairns^{2*}

1 Host Defense Discovery Performance Unit, Infectious Diseases Therapy Area Unit, Glaxosmithkline Pharmaceuticals, Upper Providence, Pennsylvania, United States of America, **2** Department of Surgery, University of North Carolina at Chapel Hill, Chapel Hill, North Carolina, United States of America, **3** Stress and Repair Discovery Performance Unit, Respiratory Therapy Area Unit, Glaxosmithkline Pharmaceuticals, Upper Merion, Pennsylvania, United States of America, **4** Division of Infectious Diseases, University of North Carolina at Chapel Hill, Chapel Hill, North Carolina, United States of America, **5** Infectious Diseases Therapy Area Unit, Glaxosmithkline Pharmaceuticals, Research Triangle Park, Durham, North Carolina, United States of America

* bruce_cairns@med.unc.edu (BAC); scott.b.berger@gsk.com (SB)



OPEN ACCESS

Citation: Eitas TK, Stepp W, Sjeklocha L, Long C, Riley C, Callahan J, et al. (2017) Differential regulation of innate immune cytokine production through pharmacological activation of Nuclear Factor-Erythroid-2-Related Factor 2 (NRF2) in burn patient immune cells and monocytes. PLoS ONE 12(9): e0184164. <https://doi.org/10.1371/journal.pone.0184164>

Editor: Paul Proost, Katholieke Universiteit Leuven Rega Institute for Medical Research, BELGIUM

Received: April 12, 2017

Accepted: August 19, 2017

Published: September 8, 2017

Copyright: © 2017 Eitas et al. This is an open access article distributed under the terms of the [Creative Commons Attribution License](https://creativecommons.org/licenses/by/4.0/), which permits unrestricted use, distribution, and reproduction in any medium, provided the original author and source are credited.

Data Availability Statement: All relevant data are within the paper and its Supporting Information files.

Funding: The project was funded by GlaxoSmithKline. The funder provided support in the form of salaries for authors (TKE, JC, YS, PG, ZH, SB), but did not have any additional role in the study design, data collection and analysis, decision to publish, or preparation of the manuscript. The

Abstract

Burn patients suffer from immunological dysfunction for which there are currently no successful interventions. Similar to previous observations, we find that burn shock patients ($\geq 15\%$ Total Burn Surface Area (TBSA) injury) have elevated levels of the innate immune cytokines Interleukin-6 (IL-6) and Monocyte Chemoattractant Protein-1 (MCP-1)/CC-motif Chemokine Ligand 2 (CCL2) early after hospital admission (0–48 Hours Post-hospital Admission (HPA)). Functional immune assays with patient Peripheral Blood Mononuclear Cells (PBMCs) revealed that burn shock patients ($\geq 15\%$ TBSA) produced elevated levels of MCP-1/CCL2 after innate immune stimulation *ex vivo* relative to mild burn patients. Interestingly, treatment of patient PBMCs with the Nuclear Factor-Erythroid-2-Related Factor 2 (NRF2) agonist, CDDO-Me(bardoxolone methyl), reduced MCP-1 production but not IL-6 or Interleukin-10 (IL-10) secretion. In enriched monocytes from healthy donors, CDDO-Me (bardoxolone methyl) also reduced LPS-induced MCP1/CCL2 production but did not alter IL-6 or IL-10 secretion. Similar immunomodulatory effects were observed with Compound 7, which activates the NRF2 pathway through a different and non-covalent Mechanism Of Action (MOA). Hence, our findings with CDDO-Me(bardoxolone methyl) and Compound 7 are likely to reflect a generalizable aspect of NRF2 activation. These observed effects were not specific to LPS-induced immune responses, as NRF2 activation also reduced MCP-1/CCL2 production after stimulation with IL-6. Pharmacological NRF2 activation reduced *Mcp-1/Ccl2* transcript accumulation without inhibiting either *Il-6* or *Il-10* transcript levels. Hence, we describe a novel aspect of NRF2 activation that may contribute to the beneficial

specific roles of these authors are articulated in the 'author contributions' section.

Competing interests: The funder provided support in the form of salaries for authors (TKE, JC, YS, PG, ZH, SB), but did not have any additional role in the study design, data collection and analysis, decision to publish, or preparation of the manuscript. The specific roles of these authors are articulated in the 'author contributions' section. TKE, JC, YS, PG, ZH, and SB are employees of GlaxoSmithKline. This commercial affiliation does not alter our adherence to PLOS ONE policies on sharing data and materials.

effects of NRF2 agonists during disease. Our work also demonstrates that the NRF2 pathway is retained and can be modulated to regulate important immunomodulatory functions in burn patient immune cells.

Introduction

Thermal injuries cause approximately 300,000 human deaths per year worldwide and are among the most expensive traumatic injuries due to long-term hospitalization and wound treatment [1, 2]. Two major aspects of burn injury are stress-associated pathophysiological changes and mis-regulated inflammatory responses. Elevated systemic levels of pro- and anti-inflammatory mediators correlate with mortality in burn patients [2], suggesting a general immunological dysfunction. Specific examples include the pro-inflammatory cytokines IL-6 and MCP-1 which associate with worse clinical outcomes [3]. Conversely, the anti-inflammatory cytokine, IL-10, has been linked with susceptibility to respiratory infections and sepsis-associated mortality [4, 5]. Hence, there is a medical need for new therapeutics that modulate host responses following burn injury [6].

In the context of disease, an important regulator of host defense against stress and inflammation is Nuclear Factor-Erythroid-2-Related Factor (NRF2). NRF2 is a transcription factor that regulates over 250 genes [7]. During periods of stress, negative regulation of NRF2 by KEAP1 (Kelch-like ECH-Associated Protein 1) is relieved, allowing NRF2 to accumulate in the cytoplasm and subsequently translocate to the nucleus and initiate a defense transcriptional program [7]. NRF2 then binds regulatory sequences known as Anti-oxidant Response Elements (AREs) or Electrophile Response Elements (EpREs) in the promoters of genes encoding anti-oxidant, cytoprotective, and phase 2 de-toxifying molecules [7]. Studies with *Nrf2*^{-/-} mice have shown that the loss of *Nrf2* alters inflammatory cytokine production such as Tumor Necrosis Factor-Alpha (TNF- α) and Interleukin 1-beta (IL-1 β) in murine fibroblasts and macrophages, respectively [8, 9]. These *in vitro* findings correlate with changes in inflammatory mediator production *in vivo* during models of sepsis, peritonitis, and burn injury [8–10]. Additionally, *Nrf2*^{-/-} deficient peritoneal macrophages produce elevated amounts of Monocyte Chemoattractant Protein-1 (MCP-1) [11].

MCP-1 was the first discovered chemokine and functions by recruiting monocytes and T cells to sites of inflammation [12]. The main receptor target for MCP-1 is C-C chemokine Receptor-2 (CCR2), which is primarily expressed on immune cells [12]. Studies have shown that monocytes/macrophages are the principle cellular sources of MCP-1 [13]. In mice, systemic MCP-1 levels are increased after thermal injury and are associated with the induction of type II T cells [14]. Clinical studies have demonstrated that elevated systemic levels of MCP-1 correlate with mortality in burn patients [3]. Hence, MCP-1 is a myeloid-associated factor that is linked to worse clinical outcomes after thermal injury.

An agonist of the NRF2 pathway is Bardoxolone methyl (CDDO-Me) [15]. CDDO-Me (bardoxolone methyl) is a synthetic triterpenoid derived from the natural product oleanic acid [16]. This small molecule functions through binding specific cysteine residues on KEAP1 and drives NRF2 protein accumulation and translocation to the nucleus [17]. CDDO-Me (bardoxolone methyl) has been shown to effectively reduce clinical outcomes in murine models of ischemic and drug-induced kidney injury [18]. Additionally, CDDO-Me (bardoxolone methyl) is currently in clinical trials for numerous indications including Pulmonary Arterial Hypertension (PAH) and Chronic Kidney Disease (CKD) but has been demonstrated to hit more

molecular targets than NRF2 [19, 20]. A recently described small molecule activator of the NRF2 pathway is Compound 7 which triggers the NRF2 pathway through blocking the interface between KEAP1 and NRF2, in a non-covalent and selective fashion [21]. Hence, both CDDO-Me (bardoxolone methyl) and Compound 7 activate the NRF2 pathway through different biochemical mechanisms [21].

In this study, we demonstrate that patients with moderate/severe ($\geq 15\%$ TBSA) or pulmonary dysfunction (< 357 SpO₂/FiO₂ ratio) have elevated levels of IL-6 and MCP-1 early (0–48 hours) after hospital admission. LPS-stimulated Peripheral Blood Mononuclear Cells (PBMCs) from moderate/severe burn patients ($\geq 15\%$ TBSA) produced elevated amounts of MCP-1 *ex vivo* indicating an altered innate immune profile. Treatment of patient PBMCs with CDDO-Me (bardoxolone methyl) effectively reduced MCP-1 production and induced the NRF2-target gene NQO1. Using enriched monocyte populations from healthy donors, we find similar immunomodulatory effects occur with multiple small molecule activators of the NRF2 pathway. NRF2 activation also reduced MCP-1 production in response to the host factor IL-6. Collectively, we demonstrate a connection between selectively activating the NRF2 pathway and inhibiting MCP-1 production that is both novel and may have important clinical implications.

Materials and methods

Patients

Patients were admitted to the North Carolina Jaycee Burn Center from November 2015 to October 2016. Following a written informed consent approved by the Institutional Review Board of the University of North Carolina at Chapel Hill School of Medicine, an initial blood sample was obtained within the first 48 hours after admission. Additional blood samples were obtained at 72–144 hours post-hospital admittance. Samples were only collected as ordered for clinical care. Clinical data including Total Burn Surface Area, age, gender, burn classification by degree, length of stay, infectious complications, organ function, and mechanical ventilation were documented throughout the duration of stay in the burn unit. HAI was defined as a positive bacterial culture from either the bloodstream or respiratory tract. SpO₂ / FiO₂ ratios were calculated at 0–24 HPA. For monocytes experiments, source leukocytes from healthy donors were ordered from Gulf Coast Regional Blood Center. The human biological samples were sourced ethically and their research use was in accord with the terms of the informed consents.

Patient blood processing

16 cc of blood was collected from burn patients or ~50 cc of blood was collected from healthy donors (Gulf Coast Regional Blood Center). Blood was overlaid onto Histopaque 1077 (Sigma, #10771) and centrifuged at 450 x g for 35 minutes. PBMCs were harvested from the interface and washed 2X with Hank's Balanced Salt Solution (HBSS) (Sigma, 55021). Cells were then subjected to Ammonium Chloride Potassium (ACK) (ThermoFisher, A1049201) lysis, filtered through a 70 μ M cell strainer (Fisher, 352350), and washed 2X with HBSS (Sigma, 55021). Cells were counted with a disposable hemocytometer (In-CYTO, C-Chip, DHC-N01).

Cell culture

5×10^5 PBMCs were plated in 200 μ L of RPMI 1640 (ThermoFisher, 1875093) with 2% Human Serum (Sigma, H3667), Beta-mercaptoethanol (Gibco, 21985–027), Sodium Pyruvate (Gibco, 11360), Non-essential Amino Acids (Gibco, 11140–076) and antibiotics (Gibco, 152140–002) in 96-well plates (Fisher, 351177). Monocyte purification was performed with

CD14 microbeads (Miltenyi, 130-050-201) according to the manufacturer's directions. Purified monocytes were re-suspended in RPMI media (See above) and plated the same as PBMCs. PBMCs and monocytes were treated with CDDO-Me (bardoxolone methyl) (Sigma-Aldrich, SMB00376), Vehicle (0.00005% DMSO), Compound 7 [21], or Vehicle (0.001% DMSO) for 1 hour before stimulation with 5 ng/mL of Lipopolysaccharide (LPS) (Sigma-Aldrich, L2630) or IL-6 (50 ng/mL, Peprotech, 200-06). At indicated times post-stimulation, plates were centrifuged at 500 x g for 5 minutes and supernatants were collected. Cell pellets were subjected to protein or RNA analysis (See below).

Immunoblot analysis

Protein lysates were generated using RIPA buffer (Sigma, R0278) with 1% SDS, 5mM DTT, Protease Inhibitor (Sigma, p8340), and Phosphatase inhibitors (Sigma-Aldrich, 490684500). Lysates were resolved on Novex 4–12% gels (Invitrogen, EC6038) and wet-transfer blotting was performed onto PVDF filter paper (Biorad, 162–01777). Membranes were blocked with 5% milk in a 1X TBST buffer (ThermoFisher, 28360) for 1 hour at room temperature. Blots were washed 3X with 1X TBST and subjected to over-night incubation at 4°C with anti-NQO1 (Abcam, ab34173) or anti-GAPDH-HRP (Cell Signaling, 3683) antibodies. Membranes were then washed 3X with 1X TBST and incubated for 1 hour at room temperature with an Peroxidase-conjugate AffiniPure Anti-Rabbit IgG antibody (Jackson ImmunoResearch, 111-035-144). Blots were washed 3X with 1X TBST and developed with Super Signal West Femto (Thermo Scientific, #34095). Chemiluminescence was measured with a Biorad Chemi-dock system. ImageJ software was used to quantify the intensity of the NQO1 bands relative to the intensity of the loading control (GAPDH). For each lane, a ratio of NQO1/GAPDH was generated and relative values were determined based on setting the NQO1/GAPDH ratio for the unstimulated, vehicle control-treated cells to 1.

RNA analysis

RNA was isolated using RNeasy Mini Kit (Qiagen, 74106) and cDNA was synthesized using SuperScript VILO Master Mix Kit (ThermoFisher, 11755050). Real time PCR was performed for *Mcp-1* (ThermoFisher, Hs00234140_m1), *Il-6* (ThermoFisher, Hs00174131_m1), *Il-10* (ThermoFisher, Hs00961622_m1), *Nqo-1* (ThermoFisher, Hs01045993_g1), *Hmox-1* (ThermoFisher, Hs00111025_m1), and *Gapdh* (ThermoFisher, Hs02758991_g1) using TaqMan Gene Expression Master Mix (ThermoFisher, 4369016). Relative target transcript expression to *Gapdh* was determined with the $2^{-\Delta\Delta CT}$ method.

Flow cytometry

$\sim 2 \times 10^6$ PBMCs or enriched monocytes (CD14⁺) were washed 2X in FACS buffer (1% PBS with 2% Fetal Bovine Serum (FBS)) before 1 hour incubation on ice with Human TruStain FcX (Biolegend, 422302) according to the manufacturer's directions. Cells were pelleted and washed 3X with FACS buffer and stained with CD11b-FITC (ebioscience, 11-0118-42) and HLA-DR-APC (Biolegend, 307610), according the manufacture's protocol. Stained cells were acquired using a LSRII Fortessa flow cytometer and analyzed with FlowJo software.

ELISA

Plasma and cellular supernatants were measured using ELISA kits for MCP-1 (BD Biosciences, 555179), IL-6 (BD Biosciences, 555220), TNF α (BD Bioscience, 555212), IL-8 (BD Biosciences, 555244), MCP-2 (CCL8) (Biolegend, 442204), and IL-10 (BD Biosciences, 555157). 1-Step

Slow TMB ELISA substrate (Thermo Scientific, 34024) and Stop Solution (Invitrogen, 5504) were used for colorimetric detection.

Statistics

Analysis of Variation (ANOVA), T-tests, Chi Square (with Fisher’s Exact Test) analysis and interpolation of cytokine values were performed with GraphPad Prism 6 Software.

Results

There were a total of 50 patients admitted that met criteria to be included in our analysis. Clinical characteristics of the burn patient cohort are shown (Table 1). The patient cohort was subdivided into mild burn injury (<15% Total Body Surface Area (TBSA) and moderate/severe burn injury (≥15% TBSA) groups (Table 1). There were not significant differences between the groups regarding age, gender, burn type, in-hospital mortality, or the occurrence of inhalation injury (Table 1). Compared to the mild burn injury group, the moderate/severe burn patient group were supported with Mechanical Ventilation (MV), susceptible to Healthcare-Associated Infections (HAIs), and had longer Length Of Stays (LOS) (Table 1, *P* < .01).

Patient blood was subjected to density gradient-based separation allowing for the isolation of plasma and PBMCs fractions. Systemic inflammatory mediators were evaluated by Enzyme Linked Immunosorbant Assay (ELISA) analysis in plasma fractions for IL-6 and MCP-1. Within the first 48 Hours Post-hospital Admittance (HPA), the moderate/severe burn injury group (≥15% TBSA) had significantly elevated levels of IL-6 and MCP-1 (Fig 1A and 1B, *P* < .0001 and *P* < .001, respectively). An important resource that is used to quantified the level of a critical ill patients’ severity of illness is the Sequential Organ Failure Assessment (SOFA) score [22]. Within the SOFA scoring system, a SpO₂/FiO₂ ratio of <357 represents dysfunction of the pulmonary compartment [23]. Independently of burn size, patients that suffered early pulmonary dysfunction (<357 SpO₂/FiO₂ ratio) at 0–24 HPA also had significantly heightened levels of IL-6 and MCP-1 (Fig 1C and 1D, *P* < .05). Longitudinal analysis of systemic IL-6 and MCP-1 levels revealed that differences between the mild (<15% TBSA) and moderate/large (≥15% TBSA) burn injury groups were most consistent early post-hospital admission (Fig 1E and 1F and S1 Fig).

Table 1. Burn patient cohort characteristics.

Characteristic	All Patients(n = 50)	<15% TBSA(n = 28)	≥15% TBSA(n = 22)	P
Age, yrs	43 ± 2	40 ± 3	47 ± 3	0.11
Female	13 (26%)	8 (29%)	5 (23%)	0.75
Flame Burn	33 (66%)	16 (57%)	17 (77%)	0.23
Scald Burn	17 (34%)	12 (43%)	5 (23%)	0.23
% TBSA	15 ± 2	4 ± 1	28 ± 2	<.001
Inhalational Injury	6 (12%)	1 (4%)	5 (23%)	0.07
In-Hospital Mortality	3 (6%)	0 (0%)	3 (14%)	0.08
Mechanical Ventilation	13 (26%)	1 (4%)	12 (55%)	<.001
HAI	10 (20%)	0 (0%)	10 (45%)	<.001
Length of Hospital Stay	18 ± 4	7 ± 1	36 ± 8	<.001

TBSA, total body surface area; HPA, hours post-hospital admittance; HAI, healthcare associated infection; ±, standard error measurement. T tests were performed for Age, TBSA, and Length of Hospital Stay. Chi Square(with Fisher’s Exact test) analysis was performed for Female, Flame Burn, Scald Burn, Inhalational Injury, Hospital Mortality, Mechanical Ventilation, and HAI.

<https://doi.org/10.1371/journal.pone.0184164.t001>

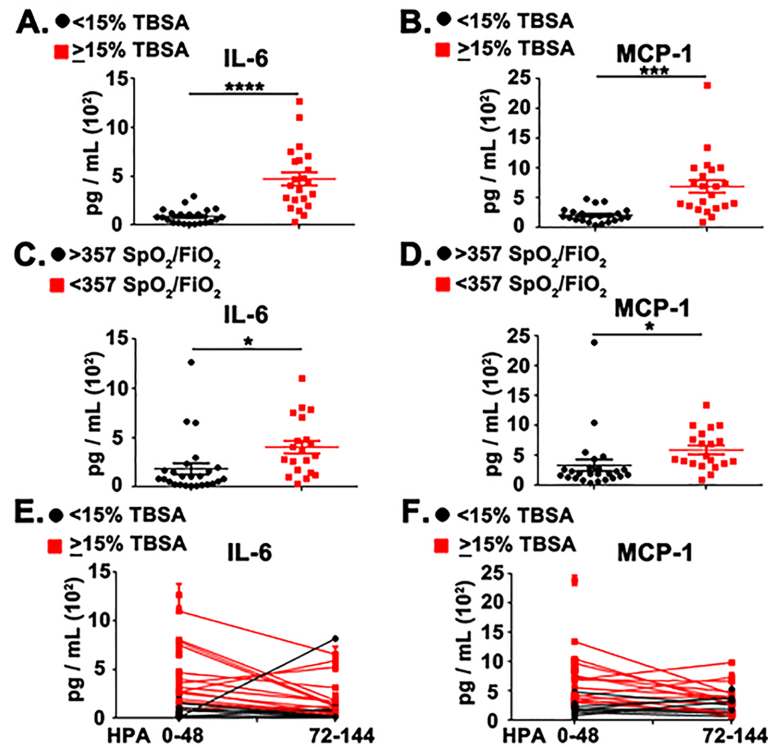


Fig 1. Systemic IL-6 and MCP-1 are elevated in patients with large burn injuries and organ dysfunction. (A) Scatter plot analysis of systemic IL-6 levels between mild (<15% TBSA, Black circles) and moderate/severe (≥15% TBSA, Red squares) patients at 0–48 HPA. (B) Scatter plot analysis of systemic MCP-1 levels between mild (<15% TBSA, Black circles) and moderate/severe (≥15% TBSA, Red squares) patients at 0–48 HPA. (C) Scatter plot analysis of systemic IL-6 levels between burn patients that suffer pulmonary distress (0–24 HPA, <357 SpO₂/FiO₂ ratio) and patients that did not (>357 SpO₂/FiO₂ ratio). (D) Scatter plot analysis of systemic MCP-1 levels between burn patients that suffer pulmonary distress (0–24 HPA, <357 SpO₂/FiO₂ ratio) and patients that did not (>357 SpO₂/FiO₂ ratio). (E) Line plot representing longitudinal analysis of systemic IL-6 accumulation from 0–48 HPA and 72–144 HPA timepoints. (F) Line plot representing longitudinal analysis of systemic MCP-1 accumulation from 0–48 HPA and 72–144 HPA timepoints. Error bars represent ± SEM. T-tests were performed to determine statistical significance for (A–D). **** represents $P < .0001$, *** represent $P < .001$, * represent $P < .05$.

<https://doi.org/10.1371/journal.pone.0184164.g001>

Since in many cases the cellular sources of IL-6 and MCP-1 are innate immune cells, we next evaluated how burn injury influenced the production of these cytokines after innate immune stimulation. Patient PBMCs were stimulated with LPS and supernatants were assayed for the production of IL-6 and MCP-1. Interestingly, the moderate/severe burn injury patient group had no difference in LPS-induced IL-6 secretion but produced more MCP-1 after innate immune stimulation (Fig 2A and 2B). We next evaluated if treatment of patient PBMCs with the NRF2 agonist, CDDO-Me (bardoxolone methyl), could lead to functional immune changes. Treatment with CDDO-Me (bardoxolone methyl) effectively reduced MCP-1 production in a concentration-dependent manner (Fig 2C). To assess if CDDO-Me (bardoxolone methyl)-mediated reduction of MCP-1 production correlated with induction of the NRF2 pathway, immunoblot analysis for NQO1 was performed. Previous studies have shown that CDDO-Me (bardoxolone methyl)-mediated induction of NQO1 is dependent on NRF2 in both murine and human cells [21]. Additionally, CDDO-Me (bardoxolone methyl)-mediated induction of NQO1 protein expression is *Nrf2*-dependent *in vivo* [15] and has been used as a pharmacodynamic marker in patient PBMCs during a phase I clinical trial [24]. Our results

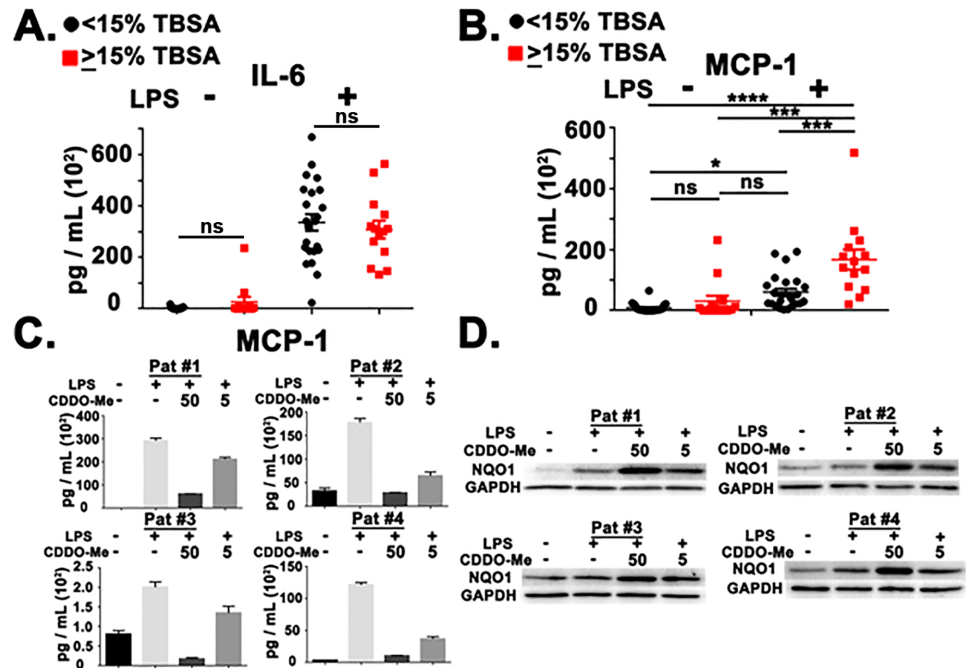


Fig 2. Pharmacological NRF2 activation reduced MCP-1 production in patient PBMCs after innate immune stimulation. (A) ELISA analysis in mild (<15% TBSA, Black circles) and moderate/severe ($\geq 15\%$ TBSA, Red squares) patient PBMCs (0–72 HPA) for IL-6 and MCP-1 in the absence (-) and presence (+) of LPS (5 ng/mL). (B) ELISA analysis in mild (<15% TBSA, Black circles) and moderate/severe ($\geq 15\%$ TBSA, Red squares) patient PBMCs (0–72 HPA) for IL-6 and MCP-1 in the absence (-) and presence (+) of LPS (5 ng/mL). (C) ELISA Analysis of 4 representative patients (#1–4) 24 hours post-LPS stimulation. CDDO-Me (bardoxolone methyl) concentrations are in 50 and 5 nM, respectively. (D) Immunoblot analysis of 4 representative patients (#1–4) at 24 hours post-LPS stimulation. CDDO-Me(bardoxolone methyl) concentrations are in 50 and 5 nM, respectively. Error bars represent \pm SEM. ANOVA analysis with Tukey post-hoc analysis was performed to determine statistical significance in A. **** = $p < .0001$. *** = $p < .001$. * = $p < .05$.

<https://doi.org/10.1371/journal.pone.0184164.g002>

demonstrate that CDDO-Me-(bardoxolone methyl) induced NQO1 accumulation in patient PBMCs in a concentration-dependent manner (Fig 2D). The intensity of NQO1 expression depicted in Fig 2D was quantified (S2 Fig).

The analysis was expanded across the burn patient cohort and we found that treatment of PBMCs with CDDO-Me(bardoxolone methyl) significantly reduced LPS-induced MCP-1 production but had no distinct effects on either IL-6 or IL-10 secretion (Fig 3A and 3C). Measurement of the percent reduction of cytokine secretion across the patient cohort revealed that CDDO-Me(bardoxolone methyl) reduced MCP-1 production to ~20% while having limited effects on LPS-induced IL-6 and IL-10 secretion (~107% and ~110%, respectively (Fig 3D)).

Since PBMCs are a heterogenous population of mononuclear immune cells (Monocytes, T cells, B cell, NK cells, etc.), we assessed if activating the NRF2 pathway could effectively modulate MCP1 production within a homogenous monocyte population. Monocytes were enriched from healthy donor PBMC populations (S3 Fig) and stimulated as was performed with patient PBMCs. ELISA analysis revealed that CDDO-Me(bardoxolone methyl) inhibited LPS-induced MCP-1 production but did not reduce IL-6 or IL-10 secretion at any of the time points measured (Fig 4A). Measurement of the percentage reduction in cytokine secretion across a set of 5 independent donors revealed that CDDO-Me(bardoxolone methyl) reduced MCP-1 production to ~15% at 16 hours post-LPS stimulation and ~30% at 24 hours post-LPS stimulation

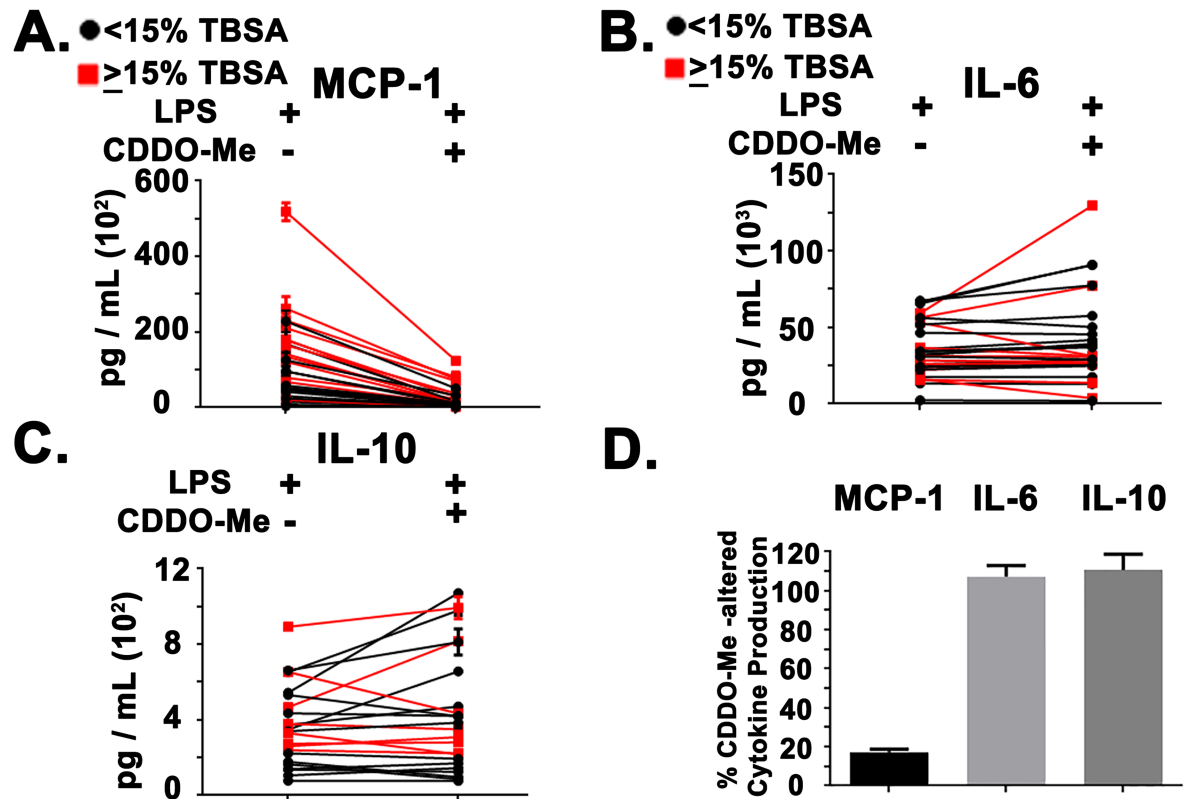


Fig 3. Pharmacological NRF2 activation reduced MCP-1 production in burn patients immune cells. (A) Line plot representing the CDDO-Me(bardoxolone methyl)(50 nM)-mediated changes in MCP-1 production across 30 patients (0–72 HPA). Red squares and lines indicate moderate/severe burn group ($\geq 15\%$ TBSA) while black circles and lines represent mild burn group ($<15\%$ TBSA). (B) Line plot representing the CDDO-Me(bardoxolone methyl)(50 nM)-mediated changes in IL-6 production across 29 patients (0–72 HPA). Red squares and lines indicate moderate/severe burn group ($\geq 15\%$ TBSA) while black circles and lines represent mild burn group ($<15\%$ TBSA). (C) Line plot representing the CDDO-Me(bardoxolone methyl) (50 nM)-mediated changes in IL-10 production across 23 patients (0–72 HPA). Red squares and lines indicate moderate/severe burn group ($\geq 15\%$ TBSA) while black circles and lines represent mild burn group ($<15\%$ TBSA). (D) Bar graph depicting the percentage of CDDO-Me(bardoxolone methyl)-altered cytokine production for MCP-1, IL-6, and IL-10. Relative values were combined across the patient cohort (N = 30 for MCP-1, N = 29 for IL-6, N = 23 for IL-10). Error bars represent \pm SEM.

<https://doi.org/10.1371/journal.pone.0184164.g003>

(Fig 4B). Additionally, CDDO-Me(bardoxolone methyl) did not reduce IL-6 or IL-10 production (Fig 4B). For both NRF2 agonists, we did observe a trend towards elevated IL-10 production at 16 hours post-LPS stimulation (Fig 4B and 4E). CDDO-Me(bardoxolone methyl) also did not reduce LPS-triggered TNF α production at 4, 8, and 16 hours post-stimulation (S4 Fig). Additionally, CDDO-Me(bardoxolone methyl) did not attenuate LPS-triggered IL-8 production but did reduce production of MCP-2 (S5 Fig). The reduction of MCP-1 correlates with induction of NQO1 expression (Fig 4C), indicating activation of the NRF2 pathway.

We next evaluated a second, independently synthesized, NRF2 agonist to determine if MCP-1 reduction was a general aspect of pharmacological NRF2 activation. Compound 7 is a new and selective small molecule activator of the NRF2 pathway that functions through blocking the KEAP1-NRF2 interface [21]. Hence, Compound 7 activates the NRF2 pathway through a different molecular Mechanism Of Action (MOA) than CDDO-Me(bardoxolone methyl). We found that Compound 7 also reduced MCP-1 production without affecting LPS-induced IL-6 or IL-10 production (Fig 4D). Measurement of the percentage reduction in cytokine secretion across 4 independent donors revealed that Compound 7 reduced MCP-1 production

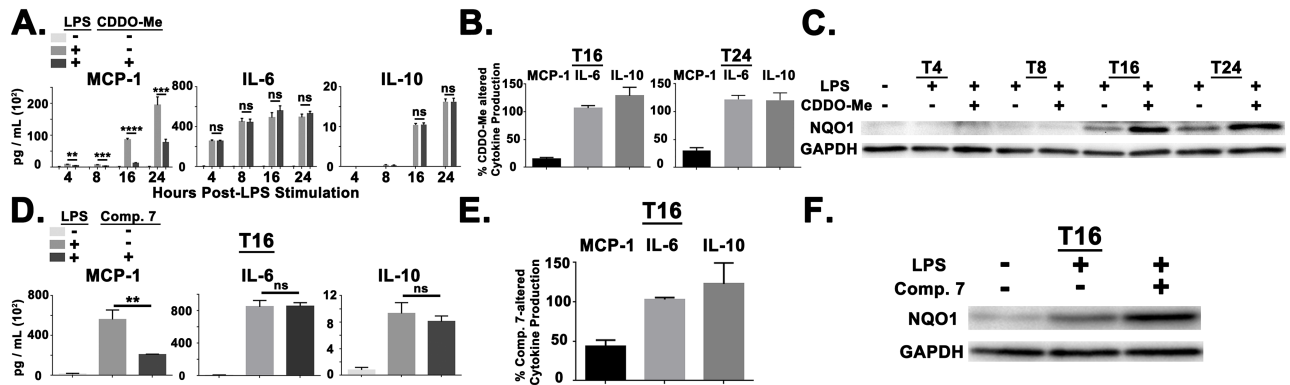


Fig 4. Multiple NRF2 agonists reduce MCP-1 production in enriched monocyte populations. (A) ELISA analysis for MCP-1, IL-6, and IL-10 in healthy donor monocytes after treatment with CDDO-Me(bardoxolone methyl) (50nM) at indicated Hours Post-LPS Stimulation (HPS). Results are representative of 5 independent donors. (B) Bar graph depicting the percentage of CDDO-Me(bardoxolone methyl)-altered cytokine production for MCP-1, IL-6, and IL-10 at 16 and 24 HPS. Relative values represent the combination of 5 independent sets of healthy donor monocytes. (C) Immunoblot analysis demonstrating the kinetics of NQO1 expression after treatment with CDDO-Me (bardoxolone methyl) (50nM). Results are representative of 5 independent donors. (D) ELISA analysis for MCP-1, IL-6, and IL-10 in healthy donor monocytes after treatment with Compound 7 (1 μM) at 16 HPS. Results are representative of 4 independent donors. (E) Bar graph depicting the percentage of Compound 7-altered cytokine production for MCP-1, IL-6, and IL-10 at 16 HPS. Relative values represent the combination of 4 independent sets of healthy donor monocytes. (F) Immunoblot analysis demonstrating NQO1 expression after treatment with Compound 7 (1 μM) at 16 HPS. Results are representative of 4 independent donors. Error bars represent SEM. ** = $p < .01$. *** = $p < .001$. **** = $p < .0001$.

<https://doi.org/10.1371/journal.pone.0184164.g004>

to ~40% at 16 hours post-LPS stimulation (Fig 4E). Additionally, inhibition of MCP-1 production by Compound 7 correlated with target engagement as measured by elevated NQO1 expression (Fig 4F).

Systemic IL-6 is elevated in burn shock patients and correlates with an increased risk of mortality [3]. *In vitro* studies have demonstrated that IL-6 can induce MCP-1 production in

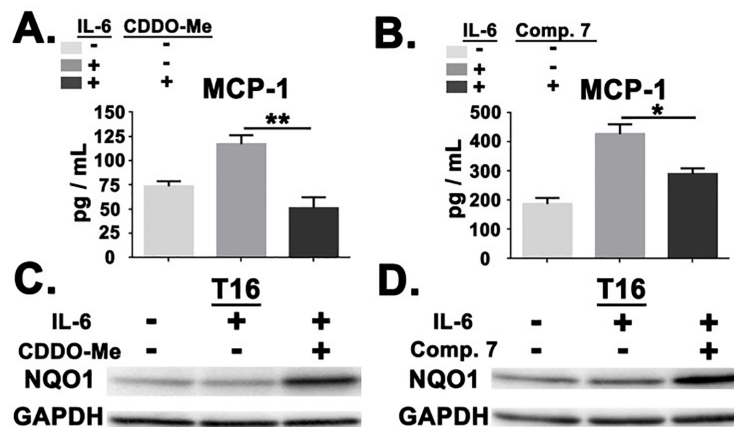


Fig 5. NRF2 activation attenuated IL-6-induced MCP-1 production. (A) ELISA analysis for MCP-1 in healthy donor monocytes after treatment with CDDO-Me(bardoxolone methyl) (50nM) at indicated Hours Post-IL-6 Stimulation (HPS). Results are representative of 4 independent donors. (B) Bar graph depicting the percentage of CDDO-Me(bardoxolone methyl)-altered MCP-1 production at 16 HPS. Relative values represent the combination of 4 independent sets of healthy donor monocytes. (C) Immunoblot analysis demonstrating NQO1 expression after treatment with CDDO-Me(bardoxolone methyl) (50nM) at 16 HPA. Results are representative of 2 independent donors. (D) ELISA analysis for MCP-1 in healthy donor monocytes after treatment with Compound 7 (1 μM) at 16 HPS. Results are representative of 2 independent donors. Error bars represent SEM. * = $p < .05$. ** = $p < .01$. *** = $p < .001$. **** = $p < .0001$.

<https://doi.org/10.1371/journal.pone.0184164.g005>

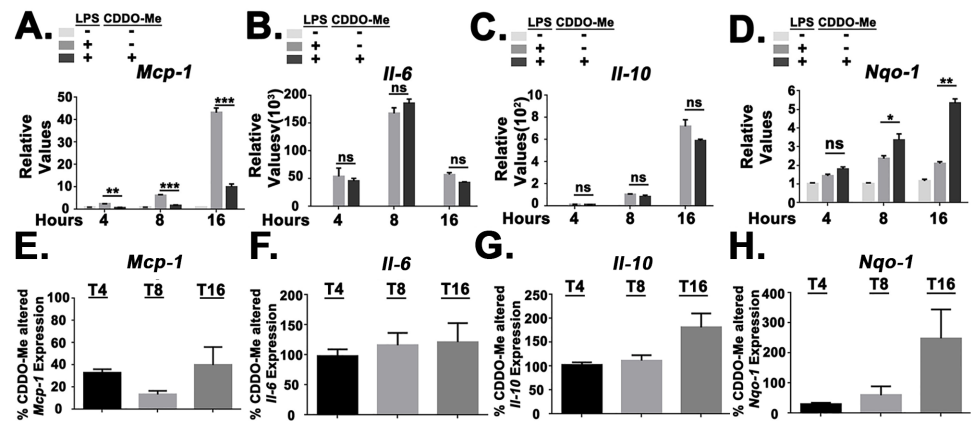


Fig 6. Pharmacological NRF2 activation inhibits *Mcp-1* transcript accumulation. (A) Real time PCR analysis for *Mcp-1* in healthy donor monocytes treated with CDDO-Me(bardoxolone methyl) (50nM). Values are relative to unstimulated, vehicle treated cells at indicated Hours Post-LPS Stimulation (HPS). Results are representative of 8 independent donors. (B) Real time PCR analysis for *Il-6* in healthy donor monocytes treated with CDDO-Me(bardoxolone methyl) (50nM). Values are relative to unstimulated, vehicle treated cells at indicated HPS. Results are representative of 6 independent donors. (C) Real time PCR analysis for *Il-10* in healthy donor monocytes treated with CDDO-Me(bardoxolone methyl) (50nM). Values are relative to unstimulated, vehicle treated cells at indicated Hours Post-LPS Stimulation (HPS). Results are representative of 6 independent donors. (D) Real time PCR analysis for *Nqo-1* in healthy donor monocytes treated with CDDO-Me(bardoxolone methyl) (50nM). Values are relative to unstimulated, vehicle treated cells at indicated HPS. Results are representative of 4 independent donors. (E) Bar graph representing the combination of CDDO-Me(bardoxolone methyl)-altered *Mcp-1* transcript accumulation in 8 donors. (F) Bar graph representing the combination of CDDO-Me(bardoxolone methyl)-altered *Il-6* transcript accumulation in 6 donors. (G) Bar graph representing the combination of CDDO-Me(bardoxolone methyl)-altered *Il-10* transcript accumulation in 6 donors. (H) Bar graph representing the combination of CDDO-Me(bardoxolone methyl)-altered *Nqo-1* transcript accumulation in 4 donors. Error bars represent SEM. * = $p < .05$. ** = $p < .01$. *** = $p < .001$. **** = $p < .0001$.

<https://doi.org/10.1371/journal.pone.0184164.g006>

human PBMCs and monocytic cell lines [25, 26]. We therefore evaluated if pharmacological NRF2 activation could attenuate IL-6-induced MCP-1 secretion in enriched monocyte populations. We found that both CDDO-Me(bardoxolone methyl) and Compound 7 reduced MCP-1 production in response to IL-6 (Fig 5A and 5B). These findings correlated with target engagement as measured by elevated NQO1 expression (Fig 5C and 5D). Unlike LPS treatment, IL-6 stimulation alone did not result in elevated NQO1 expression (Figs 4 and 5). Collectively, these results demonstrate that pharmacological NRF2 activation reduced MCP-1 production in response to both bacterial components (LPS) and host factors (IL-6) which are elevated in burn shock patients.

We next evaluated if the suppression of MCP-1 production by pharmacological NRF2 activation was due to reduced accumulation of *Mcp-1* transcript. Real time PCR analysis revealed that NRF2 activation with CDDO-Me(bardoxolone methyl) reduced *Mcp-1* transcript levels but did not inhibit LPS-induced transcript accumulation of either *Il-6* or *Il-10* (Fig 6). Additionally, the percentage reduction of LPS-induced transcript accumulation across >5 independent donors revealed that CDDO-Me(bardoxolone methyl) reduced *Mcp-1* transcript levels to ~30%, ~10%, and ~40% at 4, 8, and 16 hours post-LPS stimulation while having limited effects on *Il-6* and *Il-10* transcript accumulation, although there was trend toward higher *il-10* transcript levels at 16 hours post-LPS stimulation (Fig 6E and 6G). NRF2 activation with CDDO-Me(bardoxolone methyl) also induced *Nqo-1* expression (Fig 6D and 6H). In agreement with previously published findings [9], we found that LPS stimulation alone induced both *Nqo-1* transcript and NQO1 protein expression (Figs 4 and 6). Additionally, NRF2 activation with CDDO-Me(bardoxolone methyl) also induced *Ho-1* expression (S6 Fig).

Discussion

Patients with severe thermal injury have dysregulated immune responses which are associated with worse clinical outcomes. Burn size as represented by TBSA, is a major factor that correlates with hyper-activity of the innate immune system [27]. Additionally, burn patients with higher TBSA values are most likely to suffer from HAIs, organ failure, and mortality. Unfortunately, many therapeutic strategies targeting immune responses such as inhibitors of prostaglandin synthesis or glucocorticoids impair wound healing [28]. Hence, there is medical need for novel treatment options that target the host immune response to thermal injury.

MCP-1 is a multifaceted component of the immune system that has numerous genetic and therapeutic connections to human disease. Genetic polymorphisms in *Mcp-1* are associated with carotid intima-media thickness (atherosclerosis) in stroke patients [29]. Elevated systemic MCP-1 levels are associated with worse outcomes in patients with cardiovascular disease and thermal injury [3, 30]. Additionally, Acute Respiratory Distress Syndrome (ARDS) patients have heightened pulmonary accumulation of MCP-1 [31]. From a mechanistic standpoint, MCP-1 play a pathogenic role through recruitment of Metastasis-Associated Macrophages (MAMs) to the tumor microenvironment in breast cancer animal models [32]. In human PBMCs, MCP-1 is sufficient to promote an alternative activation (M2) profile. [26]. Therapeutically inhibiting MCP-1 synthesis leads to better clinical outcomes in animal models of sepsis and endotoxemia [33]. Importantly, biologic-based depletion strategies have shown limited efficacy in sustaining reduction of systemic MCP-1 levels in patients [34]. Hence, targeting transcriptional accumulation of *Mcp-1* through pharmacological NRF2 activation may provide unique benefit.

Both genetic and therapeutic studies have demonstrated a protective role for the NRF2 pathway during disease. Characterization of *Nrf2*^{-/-} mice have shown that the NRF2 pathway has a beneficial function in models of Acute Kidney Injury (AKI), Atherosclerosis, and Sepsis [8, 35, 36]. In response to severe burn injury, *Nrf2*^{-/-} mice suffered higher levels of mortality [10]. The elevated mortality in *Nrf2*^{-/-} mice correlated with 1) pulmonary immune cell infiltration, 2) elevated systemic levels of pro-inflammatory cytokines, and 3) intestinal permeability [10]. Additionally, *in vivo* activation of the NRF2 pathway led to improved physiological outcomes in an animal model of pulmonary hypertension [36]. In humans, genetic polymorphisms and expression of *Keap1* and *Nrf2* are associated with tumorigenesis and clinical outcomes in cancer patients [37]. Genetic polymorphisms in *Nrf2* are also associated with blood pressure and cardiovascular mortality in hemodialysis patients [38]. In the context of critical care, functional polymorphisms in *Nrf2* are associated with an increased risk for the development of Acute Lung Injury (ALI) [39]. Additionally, whole blood expression analysis from septic shock patients revealed the upregulation of 123 NRF2-modulated genes [40].

The role of the NRF2 pathway during innate immune signaling is complex due to variable host genetic systems (*Nrf2*^{-/-}, *Keap1*^{-/-}), and the usage of different small molecule activators of the NRF2 pathway (Dimethyl Fumarate, Sulforaphane, CDDO-Me (bardoxolone methyl), Compound 7, Diethylmaleate (DEM), etc.). It is imprudent to assume that pharmacological activation of the NRF2 pathway will have the opposite biological effect than *Nrf2* genetic deficiency. Using *Nrf2*^{-/-} mice, studies have shown that peritoneal macrophages and Mouse Embryonic Fibroblasts (MEFs) have enhanced NF- κ B signaling which coincided with heightened TNF α production [8, 10]. *Keap1*^{-/-} deficient mice, which have elevated NRF2 activation, have reduced transcript accumulation of *Il-6* and *Il-1 β* but not *Tnf α* in murine Bone Marrow-derived Macrophages (BMMs) [41]. Additionally, NRF2 activation with DEM (100 μ M) reduced *Il-6* and *Il-1 β* transcript accumulation in both murine BMMs and immortalized human monocyte cells (THP-1) [41]. This work also demonstrated that NRF2 activation with

DEM(100 μ M) did not alter NF- κ B p65 recruitment to the *Il-6* and *Il-1 β* promoters [41]. Alternatively, BMM from *Nrf2*^{-/-} mice produce reduced amounts of IL-1 β [9], indicating a positive role of NRF2 in promoting immune responses. TLR-induced NF- κ B signaling is required for *Nlrp3* expression and therefore subsequent NLRP3 inflammasome function [42]. Hence, further mechanistic studies are required to evaluate the relationship between NRF2 activation, innate immune cytokine production, and crosstalk with the NF- κ B pathway. It is possible that different levels of NRF2 activation may induce unique immunomodulatory effects regarding innate immune cytokine production and the NF- κ B pathway. This possibility is consistent with the findings that pharmacological NRF2 activation can induce either apoptosis or cytoprotection based on compound dosage.

In PBMCs and monocytes from sepsis patients, CDDO-Me(bardoxolone methyl) treatment did not reduce LPS-induced *Il-6* transcript accumulation although there was target engagement as measured by elevated expression of *Nqo-1* [43]. Using patient PBMCs and monocytes, we found that multiple, independently synthesized, small molecule activators of the NRF2 pathway (CDDO-Me(bardoxolone methyl), Compound 7) reduced MCP-1 production but did not reduce either IL-6 or IL-10. CDDO-Me(bardoxolone methyl) and Compound 7 target the KEAP1-NRF2 complex through different biochemical mechanisms [17, 21]. Hence, our immunological findings represent a potentially generalizable aspect of pharmacological NRF2 activation that occurs with multiple stimuli (LPS, IL-6) and is consistent across >60 individual human samples. As with many therapeutic interventions, different dosages of NRF2 agonists may lead to qualitatively different biological and/or immunomodulatory effects [44].

Small molecule agonists of the NRF2 pathway are in various stages of clinical development. Dimethyl Fumarate(Tecfidera) is an effective treatment for Multiple Sclerosis patients and has been shown to induce NRF2 activity in patients [45]. Sulforaphane is currently in a small, phase II clinical trial for the treatment of Chronic Obstructive Pulmonary Disease (NCT01335971) [46]. Finally, CDDO-Me(bardoxolone methyl) is in phase II/III clinical trials for Pulmonary Arterial Hypertension (PAH), Chronic Kidney Disease (CKD), and Type II Diabetes [47]. Hence, there is substantial precedence for targeting the NRF2 pathway during human disease.

We demonstrate that induction of the NRF2 pathway has immunological properties that could be beneficial in numerous contexts. It is worth noting that a phase III trial with CDDO-Me(bardoxolone methyl) for Chronic Kidney Disease (CKD) was terminated due to adverse cardiovascular events in a patient population with severe kidney disease [47] although there are currently ongoing phase II trials for CKD, Type II Diabetes, and Pulmonary Arterial Hypertension (PAH) (NCT02316821, NCT02036970). Therefore, there is a substantial need for additional chemical entities such as Compound 7 that induce the NRF2 pathway in a selective fashion. NRF2 agonists are currently in clinical development for chronic pulmonary and renal indications, we demonstrate that this pathway has immunomodulatory characteristics that could be beneficial in the context of severe acute illness.

Supporting information

S1 Fig. Measurement of systemic IL-6 and MCP-1 levels in burn patients at 72–144 HPA.

(A) Scatter plot analysis of systemic IL-6 levels between mild (<15% TBSA, Black circles) and moderate/severe (\geq 15% TBSA, Red squares) patients at 72–144 HPA. (B) Scatter plot analysis of systemic MCP-1 levels between mild (<15% TBSA, Black circles) and moderate/severe (\geq 15% TBSA, Red squares) patients at 72–144 HPA. Error bars represent \pm SEM. (TIF)

S2 Fig. Quantification of NQO1 expression in burn patient PBMCs. (A) Relative intensity of NQO1 expression ratio among the indicated treatment groups. Values are relative to unstimulated, vehicle-treated PBMCs for each patient. In the figure legend, values represent nM concentrations of CDDO-Me(bardoxolone methyl). Results represent the combination of the 4 patient samples shown in Fig 2D. Error bars represent \pm SEM.

(TIF)

S3 Fig. Enrichment of monocytes from a PBMC population. (A) Top. Dot plot analysis depicting Forward and Side Scatter Events (K) after CD14 microbead-mediated enrichment. Bottom. Dot plot analysis depicted expression of the monocyte markers HLA-DR and CD11b in cell populations after CD14 microbead-mediated enrichment. Results are representative of 2 independent donors.

(PNG)

S4 Fig. Pharmacological NRF2 activation does not reduce LPS-induced TNF α production.

(A) ELISA analysis for TNF α in healthy donor monocytes after treatment with CDDO-Me (bardoxolone methyl) (50nM) at indicated Hours Post-LPS Stimulation (HPS). Results are representative of 5 independent donors. (B) Bar graph depicting the percentage of CDDO-Me (bardoxolone methyl)-altered TNF α production at 4, 8, 16 HPS. Relative values represent the combination of 5 independent sets of healthy donor monocytes. Error bars represent SEM.

(TIF)

S5 Fig. Pharmacological NRF2 activation does not alter LPS-induced IL-8 production but reduces MCP-2 production.

(A) ELISA analysis for IL-8 in healthy donor monocytes after treatment with CDDO-Me(bardoxolone methyl) (50nM) at indicated Hours Post-LPS Stimulation (HPS). Results are representative of 3 independent donors. (B) Bar graph depicting the percentage of CDDO-Me(bardoxolone methyl)-altered IL-8 production at 4, 8, 16, 24 HPS. Relative values represent the combination of 3–4 independent sets of healthy donor monocytes. (C) ELISA analysis for MCP-2 in healthy donor monocytes after treatment with CDDO-Me(bardoxolone methyl) (50nM) at indicated Hours Post-LPS Stimulation (HPS). Results are representative of 7 independent donors. (D) Bar graph depicting the percentage of CDDO-Me(bardoxolone methyl)-altered MCP-2 production at 4, 8, 16, 24 HPS. Relative values represent the combination of 7 independent sets of healthy donor monocytes. ns = not significant. Error bars represent SEM. * = $p < .05$.

(TIF)

S6 Fig. Pharmacological NRF2 activation induces *Ho-1* expression. (A) Real time PCR analysis for Heme Oxygenase-1(*Ho-1*) in healthy donor monocytes treated with CDDO-Me(bardoxolone methyl) (50nM). Values are relative to unstimulated, vehicle treated cells at 16 Hours Post-LPS Stimulation (HPS). Results are representative of 2 independent donors. Error bars represent SEM. * = $p < .05$.

(TIF)

S7 Fig. Supporting information. Raw data values for all graphs.

(XLSX)

Acknowledgments

We thank the patients and staff of North Carolina Jaycee Burn Center for their participation in this study.

Author Contributions

Conceptualization: Timothy K. Eitas, Bruce Cairns.

Formal analysis: Yolanda Sanchez, Zhi Hong.

Resources: Wesley Stepp, Lucas Sjeklocha, Clayton Long, Caitlin Riley, James Callahan, Yolanda Sanchez, Laquanda Knowlin.

Supervision: Yolanda Sanchez, Peter Gough, David van Duin, Shiara Ortiz-Pujols, Samuel Jones, Robert Maile, Zhi Hong, Scott Berger, Bruce Cairns.

References

1. Peck M, Molnar J, Swart D. A global plan for burn prevention and care. *Bull World Health Organ.* 2009; 87(10):802–3. <https://doi.org/10.2471/BLT.08.059733> PMID: 19876549
2. Ruiz-Castilla M, Roca O, Masclans JR, Barret JP. RECENT ADVANCES IN BIOMARKERS IN SEVERE BURNS. *Shock.* 2016; 45(2):117–25. <https://doi.org/10.1097/SHK.0000000000000497> PMID: 26771933
3. Jeschke MG, Gauglitz GG, Finnerty CC, Kraft R, Mlcak RP, Herndon DN. Survivors versus nonsurvivors postburn: differences in inflammatory and hypermetabolic trajectories. *Ann Surg.* 2014; 259(4): 814–23. <https://doi.org/10.1097/SLA.0b013e31828dfbf1> PMID: 23579577
4. Maile R, Jones S, Pan Y, Zhou H, Jaspers I, Peden DB, et al. Association between early airway damage-associated molecular patterns and subsequent bacterial infection in patients with inhalational and burn injury. *Am J Physiol Lung Cell Mol Physiol.* 2015; 308(9):L855–60. <https://doi.org/10.1152/ajplung.00321.2014> PMID: 25770180
5. Yeh F, Lin WL, Shen HD. Changes in circulating levels of an anti-inflammatory cytokine interleukin 10 in burned patients. *Burns.* 2000; 26(5):454–9. PMID: 10812267
6. Rowan MP, Cancio LC, Elster EA, Burmeister DM, Rose LF, Natesan S, et al. Burn wound healing and treatment: review and advancements. *Crit Care.* 2015; 19(243).
7. Wakabayashi N, Slocum SL, Skoko JJ, Shin S, Kensler TW. When NRF2 talks, who's listening? *Antioxid Redox Signal.* 2010; 13(11):1649–63. <https://doi.org/10.1089/ars.2010.3216> PMID: 20367496
8. Thimmulappa RK, Lee H, Rangasamy T, Reddy SP, Yamamoto M, Kensler TW, et al. Nrf2 is a critical regulator of the innate immune response and survival during experimental sepsis. *J Clin Invest.* 2006; 116(4):984–95. <https://doi.org/10.1172/JCI25790> PMID: 16585964
9. Zhao C, Gillette DD, Li X, Zhang Z, Wen H. Nuclear factor E2-related factor-2 (Nrf2) is required for NLRP3 and AIM2 inflammasome activation. *J Biol Chem.* 2014; 289(24):17020–9. <https://doi.org/10.1074/jbc.M114.563114> PMID: 24798340
10. Chen Z, Zhang Y, Ma L, Ni Y, Zhao H. Nrf2 plays a pivotal role in protection against burn trauma-induced intestinal injury and death. *Oncotarget.* 2016;8189.
11. Ruotsalainen AK, Inkala M, Partanen ME, Lappalainen JP, Kansanen E, Mäkinen PI, et al. The absence of macrophage Nrf2 promotes early atherogenesis. *Cardiovasc Res.* 2013; 98(1):107–15. <https://doi.org/10.1093/cvr/cvt008> PMID: 23341579
12. Deshmane SL, Kremlev S, Amini S, Sawaya BE. Monocyte chemoattractant protein-1 (MCP-1): an overview. *J Interferon Cytokine Res.* 2009; 29(6):313–26. <https://doi.org/10.1089/jir.2008.0027> PMID: 19441883
13. Yoshimura T, Yuhki N, Moore SK, Appella E, Lerman MI, Leonard EJ. Human monocyte chemoattractant protein-1 (MCP-1). Full-length cDNA cloning, expression in mitogen-stimulated blood mononuclear leukocytes, and sequence similarity to mouse competence gene JE. *FEBS Lett.* 1989; 244(2):487–93. PMID: 2465924
14. Furukawa K, Kobayashi M, Herndon DN, Pollard RB, Suzuki F. Appearance of monocyte chemoattractant protein 1 (MCP-1) early after thermal injury: role in the subsequent development of burn-associated type 2 T-cell responses. *Ann Surg.* 2003; 236(1):112–9.
15. Walsh J, Jenkins RE, Wong M, Olayanju A, Powell H, Copple I, et al. Identification and quantification of the basal and inducible Nrf2-dependent proteomes in mouse liver: biochemical, pharmacological and toxicological implications. *J Proteomics.* 2014; 108:171–87. <https://doi.org/10.1016/j.jprot.2014.05.007> PMID: 24859727
16. Sporn MB, Liby KT, Yore MM, Fu L, Lopchuk JM, Gribble GW. New synthetic triterpenoids: potent agents for prevention and treatment of tissue injury caused by inflammatory and oxidative stress. *J Nat Prod.* 2011; 74(3):537–45. <https://doi.org/10.1021/np100826q> PMID: 21309592

17. Dinkova-Kostova AT, Libby KT, Stephenson KK, Holtzclaw WD, Gao X, Suh N, et al. Extremely potent triterpenoid inducers of the phase 2 response: correlations of protection against oxidant and inflammatory stress. *Proc Natl Acad Sci*. 2005; 102(12):4584–9. <https://doi.org/10.1073/pnas.0500815102> PMID: 15767573
18. Wu J, Liu X, Fan J, Chen W, Wang J, Zeng Y, et al. Bardoxolone methyl (BARD) ameliorates aristolochic acid (AA)-induced acute kidney injury through Nrf2 pathway. *Toxicology*. 2014; 318:22–31. <https://doi.org/10.1016/j.tox.2014.01.008> PMID: 24530882
19. Wang YY, Yang YX, Zhe H, He ZX, Zhou SF. Bardoxolone methyl (CDDO-Me) as a therapeutic agent: an update on its pharmacokinetic and pharmacodynamic properties. *Drug Des Devel Ther*. 2014; 8:2075–88. <https://doi.org/10.2147/DDDT.S68872> PMID: 25364233
20. Yore MM, Kettenbach AN, Sporn MB, Gerber SA, Libby KT. Proteomic analysis shows synthetic oleane triterpenoid binds to mTOR. *PLoS One*. 2011; 6(7):e22862. <https://doi.org/10.1371/journal.pone.0022862> PMID: 21818401
21. Davies TG, Wixted WE, Coyle JE, Griffiths-Jones C, Hearn K, McMennamin R, et al. Monoacidic Inhibitors of the Kelch-like ECH-Associated Protein 1: Nuclear Factor Erythroid 2-Related Factor 2 (KEAP1: NRF2) Protein-Protein Interaction with High Cell Potency Identified by Fragment-Based Discovery. *J Med Chem*. 2016; 59(8):3991–4006. <https://doi.org/10.1021/acs.jmedchem.6b00228> PMID: 27031670
22. Jones AE, Trezeciak S, Kline JA. The Sequential Organ Failure Assessment score for predicting outcome in patients with severe sepsis and evidence of hypoperfusion at the time of emergency department presentation. *Crit Care Med*. 2009; 37(5):1649–54. <https://doi.org/10.1097/CCM.0b013e31819def97> PMID: 19325482
23. Pandharipande PP, Shintani AK, Hagerman HE, St Jacques PJ, Rice TW, Sanders NW, et al. Derivation and validation of Spo2/Fio2 ratio to impute for Pao2/Fio2 ratio in the respiratory component of the Sequential Organ Failure Assessment score. *Crit Care Med*. 2009; 37(4):1317–21. <https://doi.org/10.1097/CCM.0b013e31819cefa9> PMID: 19242333
24. Hong DS, Kurzrock R, Supko JG, He X, Naing A, Wheler J, et al. A phase I first-in-human trial of bardoxolone methyl in patients with advanced solid tumors and lymphomas. *Clin Cancer Res*. 2012; 18(12):3396–406. <https://doi.org/10.1158/1078-0432.CCR-11-2703> PMID: 22634319
25. Biswas P, Delfanti F, Bernasconi S, Mengozzi M, Cota M, Polentarutti N, et al. Interleukin-6 induces monocyte chemotactic protein-1 in peripheral blood mononuclear cells and in the U937 cell line. *Blood*. 1998; 91(1):258–65. PMID: 9414293
26. Roca H, Varsos ZS, Sud S, Craig MJ, Ying C, Pienta KJ. CCL2 and interleukin-6 promote survival of human CD11b+ peripheral blood mononuclear cells and induce M2-type macrophage polarization. *J Biol Chem*. 2009; 284(49):34342–54. <https://doi.org/10.1074/jbc.M109.042671> PMID: 19833726
27. Jeschke MG, Micak RD, Finnerty CC, Norbury WB, Gauglitz GG, Kulp GA, et al. Burn size determines the inflammatory and hypermetabolic response. *Crit Care*. 2007; 11(4):R90. <https://doi.org/10.1186/cc6102> PMID: 17716366
28. Franz MG, Steede DL, Robson MC. Optimizing healing of the acute wound by minimizing complications. *Curr Probl Surg*. 2007; 44:691–763. <https://doi.org/10.1067/j.cpsurg.2007.07.001> PMID: 18036992
29. Brenner D, Labreuche J, Touboul PJ, Schmidt-Petersen K, Poirier O, Perret C, et al. Cytokine polymorphisms associated with carotid intima-media thickness in stroke patients. *Stroke*. 2006; 37(7):1691–6. <https://doi.org/10.1161/01.STR.0000226565.76113.6c> PMID: 16741188
30. Martín-Ventura JL, Blanco-Colio LM, Tuñón J, Muñoz-García B, Madrigal-Matute J, Moreno JA, et al. Biomarkers in cardiovascular medicine. *Rev Esp Cardiol* 2009; 62(6):677–88. PMID: 19480764
31. Rosseau S, Hammerl P, Maus U, Walmrath HD, Schütte H, Grimminger F, et al. Phenotypic characterization of alveolar monocyte recruitment in acute respiratory distress syndrome. *Am J Physiol Lung Cell Mol Physiol*. 2000; 279(1):L25–35. PMID: 10893199
32. Kitamura T, Qian BZ, Soong D, Cassetta L, Noy R, Sugano G, et al. CCL2-induced chemokine cascade promotes breast cancer metastasis by enhancing retention of metastasis-associated macrophages. *J Exp Med*. 2015; 212(7):1043–59. <https://doi.org/10.1084/jem.20141836> PMID: 26056232
33. Ramnath RD, Ng SW, Guglielmotti A, Bhatia M. Role of MCP-1 in endotoxemia and sepsis. *Int Immunopharmacol*. 2008; 6:810–8.
34. Pienta KJ, Machiels JP, Schrijvers D, Alekseev B, Shkolnik M, Crabb SJ, et al. Phase 2 study of carlumab (CNTO 888), a human monoclonal antibody against CC-chemokine ligand 2 (CCL2), in metastatic castration-resistant prostate cancer. *Invest New Drugs*. 2013; 31(3):760–8. <https://doi.org/10.1007/s10637-012-9869-8> PMID: 22907596
35. Shelton LM, Park PK, Coppole IM. Role of Nrf2 in protection against acute kidney injury. *Kidney Int*. 2013; 84(6):1090–5. <https://doi.org/10.1038/ki.2013.248> PMID: 23783243

36. Eba S, Hoshikawa Y, Moriguchi T, Mitsuishi Y, Satoh H, Ishida K, et al. The nuclear factor erythroid 2-related factor 2 activator oltipraz attenuates chronic hypoxia-induced cardiopulmonary alterations in mice. *Am J Respir Cell Mol Biol*. 2013; 49(2):324–9. <https://doi.org/10.1165/rcmb.2011-0396OC> PMID: 23590302
37. Ishikawa T. Genetic polymorphism in the NRF2 gene as a prognosis marker for cancer chemotherapy. *Front Genet*. 2014; 5(383).
38. Shimoyama Y, Mitsuda Y, Tsuruta Y, Hamajima N, Niwa T. Polymorphism of Nrf2, an antioxidative gene, is associated with blood pressure and cardiovascular mortality in hemodialysis patients. *Int J Med Sci*. 2014; 11(7):726–31. <https://doi.org/10.7150/ijms.8590> PMID: 24904228
39. Marzec JM, Christie JD, Reddy SP, Jedlicka AE, Vuong H, Lanken PN, et al. Functional polymorphisms in the transcription factor NRF2 in humans increase the risk of acute lung injury. *FASEB J* 2007; 21(9): 2237–46. <https://doi.org/10.1096/fj.06-7759com> PMID: 17384144
40. Grunwell JR, Weiss SL, Cvijanovich NZ, Allen GL, Thomas NJ, Freishtat RJ, et al. Differential expression of the Nrf2-linked genes in pediatric septic shock. *Crit Care*. 2015; 19(327).
41. Kobayashi EH, Suzuki T, Funayama R, Nagashima T, Hayashi M, Sekine H, et al. Nrf2 suppresses macrophage inflammatory response by blocking proinflammatory cytokine transcription. *Nat Commun*. 2016; 7(11624).
42. Bauernfeind FG, Horvath G, Stutz A, Alnemri ES, MacDonald K, Speert D, et al. Cutting edge: NF-kappaB activating pattern recognition and cytokine receptors license NLRP3 inflammasome activation by regulating NLRP3 expression. *J Immunol*. 2009; 183(2):787–91. <https://doi.org/10.4049/jimmunol.0901363> PMID: 19570822
43. Noel S, Z L Navas-Acien A, Fuchs RJ. The effect of ex vivo CDDO-Me activation on nuclear factor erythroid 2-related factor 2 pathway in white blood cells from patients with septic shock. *Shock*. 2014; 42(5):392–9. <https://doi.org/10.1097/SHK.0000000000000236> PMID: 25105464
44. Liby Karen T. S MB. Synthetic Oleanane Triterpenoids: Multifunctional Drugs with a Broad Range of Applications for Prevention and Treatment of Chronic Disease. *Pharmacol Rev*. 2012; 64(4):972–1003. <https://doi.org/10.1124/pr.111.004846> PMID: 22966038
45. Gopal S, Mikulshis A, Gold R, Fox RJ, Dawson KT, Amaravadi L. Evidence of activation of the Nrf2 pathway in multiple sclerosis patients treated with delayed-release dimethyl fumarate in the Phase 3 DEFINE and CONFIRM studies. *Mult Scler*. 2017; ePub.
46. Wise RA, Holbrook JT, Criner G, Sethi S, Rayapudi S, Sudini KR, et al. Broccoli Sprout Extract Trial Research Group. Lack of Effect of Oral Sulforaphane Administration on Nrf2 Expression in COPD: A Randomized, Double-Blind, Placebo Controlled Trial. *PLoS One*. 2016; 11(11):e0163716. <https://doi.org/10.1371/journal.pone.0163716> PMID: 27832073
47. Suzuki T, Motohashi H, Yamamoto M. Toward clinical application of the Keap1-Nrf2 pathway. *Trends Pharmacol Sci*. 2013; 6:340–6.